

## Supporting information

### **Microfluidic-assisted Sol-gel Preparation of Monodisperse Mesoporous Silica Microspheres with Controlled Size, Surface Morphology, Porosity and Stiffness**

Zhang Dai<sup>1</sup>, Yue Liu<sup>1</sup>, Yahui Liu<sup>1</sup>, Xiuling Jiao<sup>1</sup>, Dairong Chen<sup>1</sup>, Ningji Gong<sup>2\*</sup> and Ting Wang<sup>1\*</sup>

1. National Engineering Research Center for Colloidal Materials, School of Chemistry & Chemical Engineering, Shandong University, Jinan 250100, P. R. China

2. Department of Emergency, The Second Hospital, Cheeloo College of Medicine, Shandong University, Jinan, Shandong, 250033, P. R. China

E-mail: [t54wang@sdu.edu.cn](mailto:t54wang@sdu.edu.cn), [gongningji@sdu.edu.cn](mailto:gongningji@sdu.edu.cn)

### **1. Experimental and section**

#### 1.1 Material

Tetraethyl orthosilicate (TEOS) was purchased from Sinoreagent Chemistry (China). Ethanol was purchased from Aladdin (China). Hydrochloric acid was purchased from Sinopharm Chemical Reagent Co., LTD. ABIL EM 90 was purchased from Xingkaiyue (China). Hexadecane were purchased from Macklin (China). All chemicals of analytical grade were used as received without any purification. Pure water was generated by an ELGA purelab system, with a resistance greater than 18.2 M $\Omega$ ·cm at 25°C.

#### 1.2 Characterization

Scanning electron microscopy (SEM, AEISS SUPRA55) and transmission electron microscopy (TEM, JEM-1011) were used to characterize the morphology of nanoparticles in the sol and the prepared microspheres. The TEM samples were prepared using the solution dispersion method. All samples were prepared under identical conditions; prior to sampling, the sol was subjected to ultrasonication for 30 minutes. Subsequently, a small amount of the sol was dropped onto a microgrid copper mesh and allowed to dry at room temperature for 15 minutes. Viscosity of the precursor sol were measured on a rheometer (MCR302, Anton Paar GmbH, Graz, Austria) with an angular frequency of 10 rad·s<sup>-1</sup>. After diluting the precursor sol to neutral, the surface

potential of the nanoparticles in the sol was measured by zeta potential analyzer (Nano ZS, Malvern, England). X-ray diffraction (XRD) data were collected on the Rigaku D/Max 2200 pc diffractometer. The  $^{29}\text{Si}$  NMR was carried out by an Advance III HD M 400 M.

### 1.3 Simulations and theoretical analysis the microfluidic device

In order to better understand and explain convection in fluid, considering that the range of convection is mainly determined by fluid mode in microfluidic channel, we considered an additional dimensionless parameter Reynolds number (Re)<sup>1</sup>. The expression for the Reynolds number is:

$$Re = \frac{\rho UL}{\mu}$$

Where  $\rho$  is the density of the fluid ( $\text{kg/m}^3$ ),  $U$  is the average velocity of the fluid (m/s),  $L$  is the characteristic length of the microchannel (m), and  $\mu$  is the dynamic viscosity of the fluid ( $\text{Pa}\cdot\text{s}$ ). Through the formula, we calculate that the Re value of the fluid in the microchannel is 2.67, which is much smaller than the critical Reynold's number 2000 of unstable turbulence. The preparation of microfluidic droplet is always laminar flow, and no turbulence phenomenon occurs, thus ensuring the stability of the prepared droplet.

Based on the cross channel model with liquid stress shear, the finite element droplet shear behavior of continuous and dispersed phases is simulated. We use the volume of fluid (VOF) method to simulate two immiscible fluids by solving separate momentum equations and dealing with the volume ratio of each fluid passing through a region. In the two-phase flow motion in a microchannel, the momentum equation of each phase is consistent with the momentum equation in the whole region, and momentum equation of the two-phase flow are as follows<sup>2, 3</sup>:

$$\frac{\partial(\rho \mathbf{v})}{\partial t} + \nabla(\rho \mathbf{v} \mathbf{v}) = -\nabla p + \nabla[\mu(\nabla \mathbf{v} + \nabla \mathbf{v}^T)] + \mathbf{F}$$

where  $\rho$ ,  $t$ ,  $\mathbf{v}$ ,  $p$  and  $\mu$  represent density, time, velocity, pressure and viscosity, respectively.  $\mathbf{F}$  is a momentum source. The equations above are related with the volume fraction,  $\alpha_i$ , of each component phase through the density,  $\rho$  and the viscosity,  $\mu$ . The properties in each computational grid cell are represent of either a pure phase or

a mixture of phases.

The horizontal inlet of the pipeline is the sol inlet, and the two perpendicular entrances on both sides are the oil phase inlet, both of which are the flow rate inlet boundary conditions, and the outlet adopts the free flow boundary conditions. The experimental temperature was set at 300K, and the influence of gravity, pipeline, liquid and surface tension of liquid and liquid were not considered. FLUENT software was used for simulation.

#### 1.4 In-situ droplet shrinkage observation

In situ observations of droplet shrinkage and gelation were conducted using an optical microscope equipped with a camera (GP-52, Kunshan, China) and a specially designed temperature-controlled stage. Temperature regulation was achieved with a precision of  $\pm 1^\circ\text{C}$  via a dedicated controller. The droplets generated by the microfluidic chip were immediately collected into a 2 cm diameter container secured on a heating stage. To preserve the monodispersity of the droplets, 1 ml of the oil phase was pre-added to the container. The temperature settings were systematically maintained at  $30^\circ\text{C}$ ,  $50^\circ\text{C}$ , and  $70^\circ\text{C}$ , with the droplet morphology being documented by the microscope at 5 min intervals. The majority of image processing was performed using ImageJ software.

#### 1.5 Surface area (BET) measurement

For surface measurements, the sample is placed in an atmosphere of nitrogen gas. The sample was inserted into a Dewar vacuum flask filled with liquid nitrogen for nitrogen adsorption. Subsequent removal from the coolant results in nitrogen desorption at room temperature. The BET specific surface area, specific surface area, micropore volume and micropore area of the sample were calculated by nitrogen adsorption curve analysis. The test pressure is 0.05-0.95 bar and the isotherm is measured at  $-196^\circ\text{C}$  (Quantachrome Autosorb IQ)

#### 1.6 AFM mechanical test

Quantitative nanomechanical information of the sample was characterized by Atomic force microscopy (AFM, BioScope Resolve). The mechanical information of the probe tip and the sample was measured by atomic force microscopy. Under the

action of external load  $F$ , the AFM tip is pressed into a certain depth on the surface of the silica ball. In order to quantitatively extract the elasticity modulus from the force indentation curve, the classical Hertzian contact model in contact continuum mechanics is applied. The calculation equation of the model is<sup>4, 5</sup>:

$$F_{cone} = \frac{2}{\pi} \tan \alpha E^* \delta^2$$

where  $\alpha$  is the half-opening angle of the conical tip (value given by the manufacturer  $15^\circ$ ), respectively, the radius of curvature of the spherical or paraboloid indenter and of the indented particles, and  $1/E^* = (1 - \nu_1^2)/E_1 + (1 - \nu_2^2)/E_2$ , where  $E_1$  and  $E_2$  are the surface elastic modulus and  $\nu_1$  and  $\nu_2$  are the Poisson ratios of the tip and of the sample, respectively.  $\delta$  is equal to the depth of indentation on the surface to the tip.

### 1.7 Preparation for the SiO<sub>2</sub> microspheres

Firstly, deionized water, ethanol (99.9% purity), and tetraethyl orthosilicate (TEOS) are thoroughly mixed at room temperature to achieve a homogeneous solution with a mass ratio of 6.5 TEOS: 6 H<sub>2</sub>O: 4 ethanol. Subsequently, the pH of the solution is carefully adjusted to approximately 2 using 1 M HCl. After stirring for 12 h, TEOS was fully hydrolyzed. So that the sol to maintain a low pH value and slow gelation. To effectively modulate the properties of nanoparticles within the sol, we prepared TEOS precursors with varying mass fractions, with a compilation of all sample compositions presented in Table S1. Furthermore, we prepared a continuous oil phase fluid by dissolving the double-block copolymer non-ionic surfactant ABIL EM 90 in hexadecane at a concentration of 5 wt%.

The prepared aqueous precursor solution and the oil phase were loaded into two 50 mL reservoir cells, which were then fixed to a tabletop microfluidic device (JDF05, NanoInstrument). The microfluidic chip is predominantly constructed from polydimethylsiloxane (PDMS) and glass. The fabrication process commences with the creation of microchannels in PDMS via photolithography. Subsequently, the PDMS and glass components are irreversibly sealed through plasma-assisted bonding. The two reservoir cells were connected to an air pump, and have established the flow rate of the silica precursor solution (dispersed phase) at 5  $\mu$ l/min, while modulating the flow rate

of the corresponding oil phase (continuous phase) within the range of 5 to 50  $\mu\text{l}/\text{min}$  to gradually change the volume flow rate ratio of the continuous phase to the dispersed phase ( $V_C/V_D$ ) from 1:1 to 4:1, 6:1, 8:1, and ultimately to 10:1. The emulsification of the TEOS precursor was accomplished using two digitally controlled FluidicLab pneumatic pumps, which supplied the sol-water phase and the oil-containing continuous phase to the microfluidic device. The collected precursor droplets underwent precondensation at  $70^\circ\text{C}$  and for removing the oil phase involved dispersing the precondensation microspheres in diethyl ether, followed by centrifugal washing twice to thoroughly remove the oil phase. Subsequently, the microspheres were washed twice with ethanol using the same procedure, and then dried in a vacuum oven at  $70^\circ\text{C}$  for 4 hours. The physical properties of the microspheres after pre-curing were stable and did not change with washing. Compared to washing, the sintering temperature has a more significant impact on the physical properties of the microspheres. Subsequently, the samples were heated to  $200^\circ\text{C}$  in an air atmosphere at a rate of  $5^\circ\text{C}$  per minute for a duration of 1 hour, after which the temperature was incrementally increased to  $800^\circ\text{C}$  at the same heating rate. To achieve impurity-free mesoporous silica microspheres (MSMs), the samples were held at  $800^\circ\text{C}$  for 4 hours and then permitted to cool naturally to ambient temperature.

The transformation from prepared droplets to silica microspheres necessitates passing through several stages, including pre-gelation, washing, drying, and calcination. The pre-gelation process takes approximately 4 hours, the washing process requires 1 hour, and subsequent drying after washing takes 4 hours. Finally, the calcination process, which may last up to 10 hours, is carried out. In total, the entire procedure spans approximately 20 hours. The overall production rate of microspheres, taking the droplet preparation rate of the PDMS-G-60 chip as an example, is ultimately  $75\text{ mg/h}$ , considering the unavoidable losses during collection and washing in the actual production process.

Table S1 Synthesis parameters of the silica sol prepared in this work.

Sample	TEOS	H <sub>2</sub> O	Ethanol	HCl
Si <sub>TEOS10 wt%</sub> , W/E=6:4	1.1 g	6 g	4 g	0.008 g
Si <sub>TEOS20 wt%</sub> , W/E=6:4	2.5 g	6 g	4 g	0.008 g
Si <sub>TEOS30 wt%</sub> , W/E=6:4	4.3 g	6 g	4 g	0.01 g
Si <sub>TEOS40 wt%</sub> , W/E=6:4	6.5 g	6 g	4 g	0.01 g
Si <sub>TEOS40 wt%</sub> , W/E=4:6	6.5 g	4 g	6 g	0.01 g
Si <sub>TEOS40 wt%</sub> , W/E=8:2	6.5 g	8 g	2 g	0.01 g

Table S2 The details of the microfluidic chip.

Model number	PDMS-G-30	PDMS-G-60	PDMS-G-100
Chip width (mm)		75*25*2	
Width of flow (μm)	30~250	50~350	100~700
Notch width (μm)	30	60	100
Droplet diameter (μm)	21~42	37~63	56~103
Filling volume (μL)	0.46	2.82	11.05

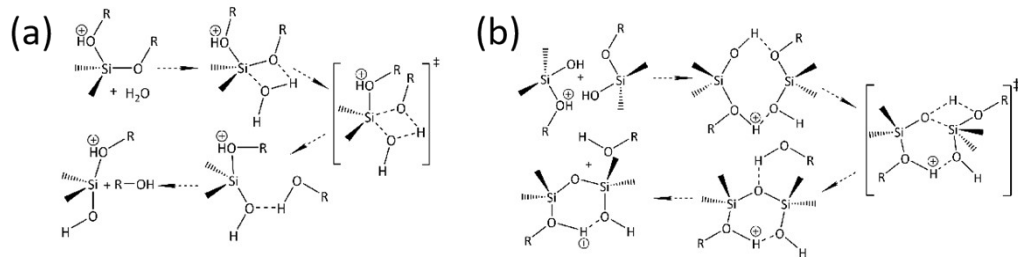
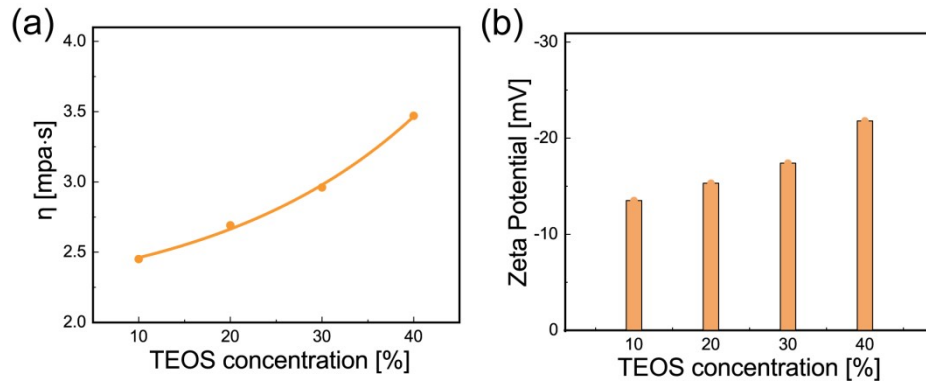
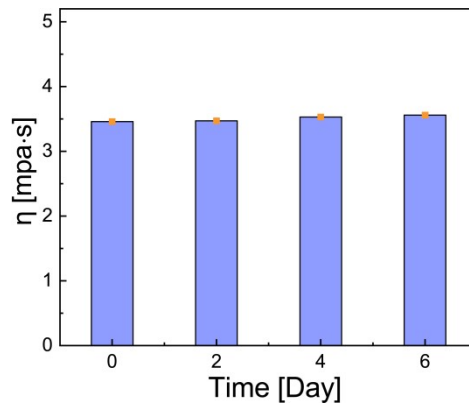


Fig. S1 Pentadentate theory of hydrolysis and condensation. (a) hydrolysis. (b) condensation.



**Fig. S2** (a) the viscosity changes of sol with different TEOS content and (b) Zeta Potential.



**Fig. S3** The change of sol viscosity with time.

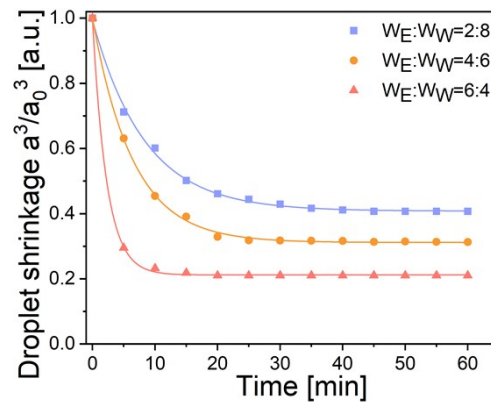


**Fig. S4** The droplet shrinkage with different ratio of alcohol to water.

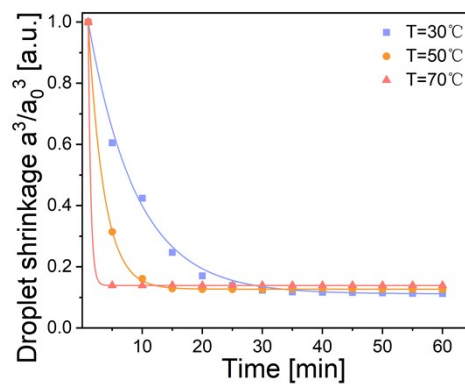


**Fig. S5** The droplet shrinkage with different temperature.

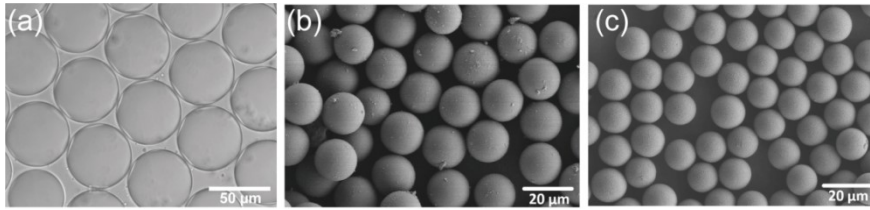


**Fig. S6** (a) Micro droplets. (b) Gelled microspheres. (c) Annealed microspheres.

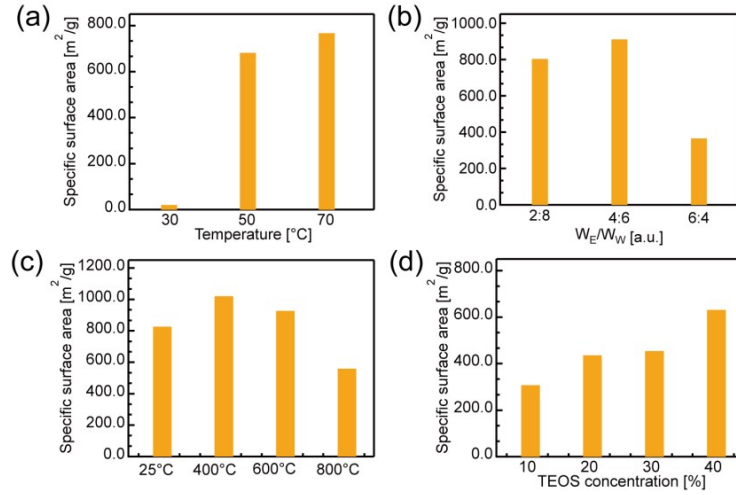


**Fig. S7** Specific surface area of the microsphere. (a) gelation temperature. (b) Different alcohol to water ratio. (c) Different annealing temperature. (d) Different TEOS content.

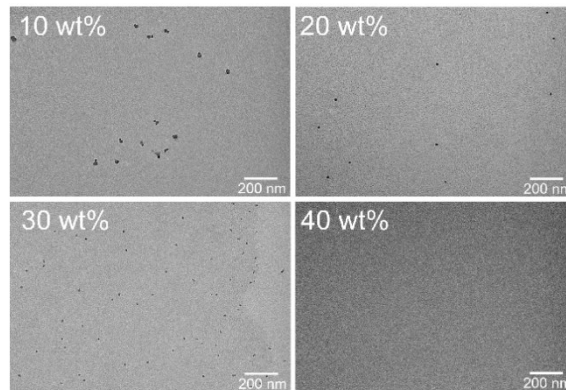


**Fig. S8** TEM with different TEOS concentrations.

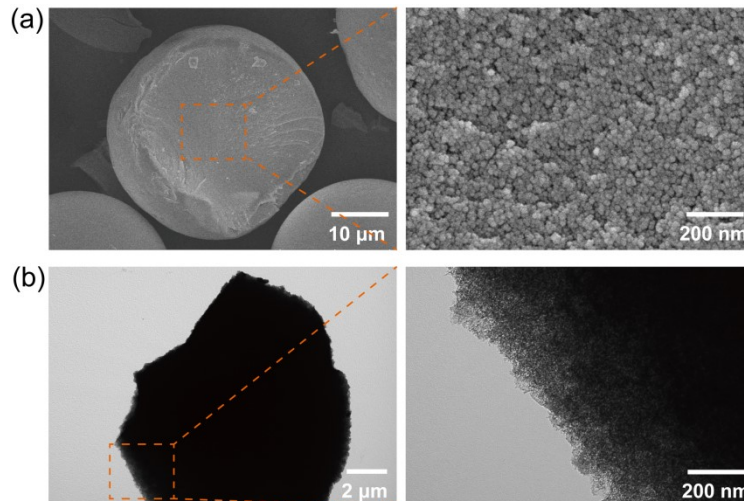




**Fig. S9** (a) SEM and (b) TEM images of the microsphere cross-sections.

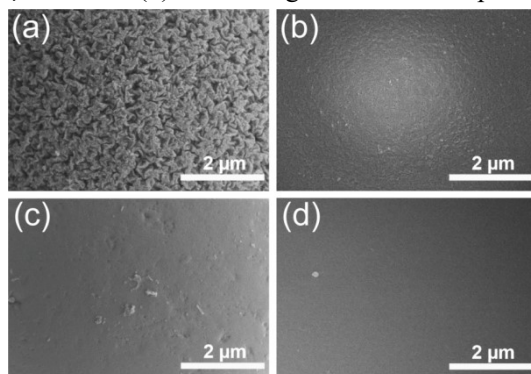


**Fig. S10** SEM of microsphere surface morphology. (a)  $W_{\text{TEOS}}=10\%$ . (b)  $W_{\text{TEOS}}=20\%$ . (c)  $W_{\text{TEOS}}=30\%$ . (d)  $W_{\text{TEOS}}=40\%$ .

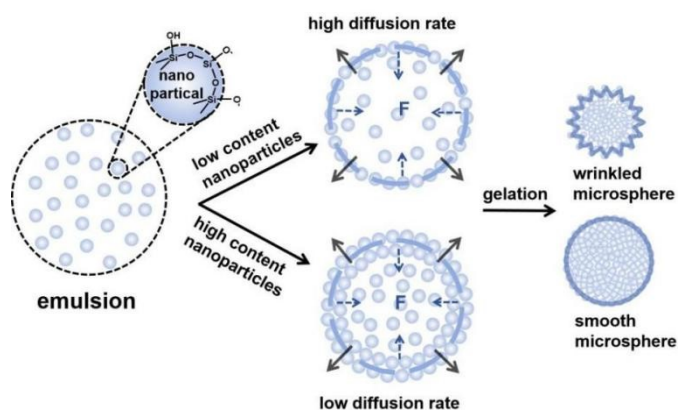


**Fig. S11** Microsphere contraction diagram.

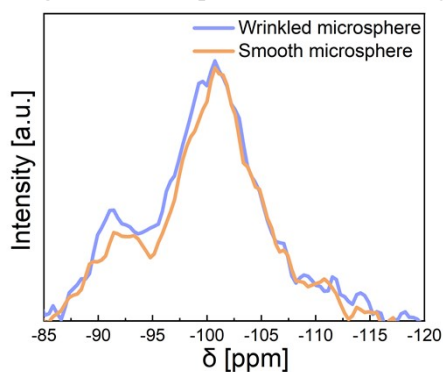


**Fig. S12** The  $^{29}\text{Si}$  NMR spectra of wrinkled microsphere and smooth.

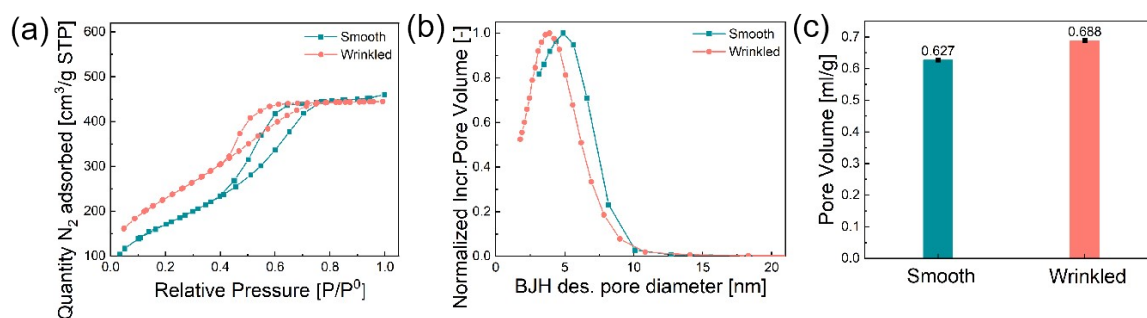


**Fig. S13.** (a)  $\text{N}_2$  adsorption and desorption curves, (b) pore size and (c) porosity of wrinkled and smooth microspheres.

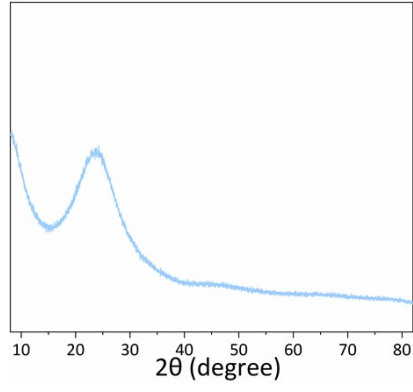


**Fig. S14** XRD of silica microspheres annealed at 800 °C for 4 h.

## Reference

1. N. Hao, Y. Nie and J. X. J. Zhang, *Biomater. Sci.*, 2019, **7**, 2218-2240.
2. Z. Yang, X. Ma, S. Wang and D. Liu, *Chem. Eng. Sci.*, 2022, **255**, 117683.
3. M. Azarmanesh, M. Farhadi and P. Azizian, *Phys. Fluids*. 2016, **28**, 032055.
4. S. Armini, I. U. Vakarelski, C. M. Whelan, K. Maex, *LANGMUIR*, 2007, **23**, 2007-2014.
5. H. Gojzewski, J. Obszarska, A. Harlay, M. A. Hempenius and G. J. Vancso, *Polymer*, 2018, **150**, 289-300.